

An object correlation and maneuver detection approach for space surveillance

Jian Huang¹, Wei-Dong Hu¹, Qin Xin² and Xiao-Yong Du¹

¹ ATR Key Lab., College of Electronic Science and Engineering, National University of Defense Technology, Changsha 410073, China; huangjian@nudt.edu.cn

² Faculty of Science and Technology, University of the Faroe Islands, Torshavn, FO100, Faroe Islands

Received 2012 March 25; accepted 2012 April 12

Abstract Object correlation and maneuver detection are persistent problems in space surveillance and maintenance of a space object catalog. We integrate these two problems into one interrelated problem, and consider them simultaneously under a scenario where space objects only perform a single in-track orbital maneuver during the time intervals between observations. We mathematically formulate this integrated scenario as a maximum a posteriori (MAP) estimation. In this work, we propose a novel approach to solve the MAP estimation. More precisely, the corresponding posterior probability of an orbital maneuver and a joint association event can be approximated by the Joint Probabilistic Data Association (JPDA) algorithm. Subsequently, the maneuvering parameters are estimated by optimally solving the constrained non-linear least squares iterative process based on the second-order cone programming (SOCP) algorithm. The desired solution is derived according to the MAP criterions. The performance and advantages of the proposed approach have been shown by both theoretical analysis and simulation results. We hope that our work will stimulate future work on space surveillance and maintenance of a space object catalog.

Key words: celestial mechanics — methods: analytical — techniques: miscellaneous — surveys

1 INTRODUCTION

Object correlation and maneuver detection are very challenging and persistent problems for space surveillance tasks. It is known that there are currently at least 19 000 trackable objects in Earth orbit and among them 1300 have the capability of performing mission objectives and/or orbital maintenance (Holzinger & Scheeres 2010). Moreover, these numbers are expected to grow significantly due to increased tracking capabilities and new launches. In order to satisfy the requirements of space situational awareness and collision avoidance, these orbiting objects should be under continuous surveillance, however, maintaining a catalog of these objects is a very challenging task. In addition, the available observations collected by the space surveillance systems are generally discrete in the spatial-temporal domain. Therefore, the problem of object correlation and maneuver detection during the time intervals between these observations becomes much more difficult, in contrast with that

commonly encountered in real-time tracking applications, particularly in regions of space that have high-densities of spacecraft.

Object correlation and maneuver detection have been well studied in the literature. Regarding object correlation, Tommei et al. (2007) solved the problem of orbital determination and correlation of space debris by using the admissible regions and virtual debris algorithm, which can also be applied to optical and radar observations. By embedding the admissible regions into the Delaunay space, Maruskin et al. (2009) presented a notional algorithm for computing an orbital correlation and determination between two uncorrelated tracks. Farnocchia et al. (2010) described two different linkage methods, i.e. the virtual debris algorithm and the Keplerian integral method, which aim at implementation with affordable computational complexity. Regarding the problem of maneuver detection, the corresponding methods are the varieties with respect to different modes of orbital maneuvering and detection metrics. Storch (2005) estimated the maneuvering parameters of a collocated satellite in geosynchronous orbit by using nonlinear least squares. In Patera (2008), the energy per unit mass was computed to detect a space event based on the technique of a moving window curve fit. Holzinger & Scheeres (2010) presented an object correlation and maneuver detection method using optimal control performance metrics. Kelecy & Jah (2010) focused on the detection and reconstruction of single low thrust in-track maneuvers by using the orbit determination strategies based on the batch least-squares and extended Kalman filter (EKF). Generally speaking, the aforementioned methods separately handled the problems of object correlation and maneuvering. Moreover, these algorithms can neither accurately reconstruct the parameters of orbital maneuvers, nor provide an estimation of confidence for the correct correlation between objects.

However, in practical applications, object correlation and maneuver detection are interrelated. Orbital maneuvering is a significant factor leading to uncorrelated tracks. In addition, uncorrelated tracks themselves lead to intractability in the detection and calculation of orbital maneuvers. Therefore, it is necessary to solve the problem of space object correlation and orbital maneuvering simultaneously. In addition, not only the decisions for maneuver detection and object correlation are necessary, but also detailed information about events, e.g. when and where the orbital maneuver occurs, whether the reconstructed maneuver event is feasible in application, and the confidence of correlation, are all needed in order to arrive at the desired solutions.

Space objects can maneuver in several modes. According to the corresponding types of thrust (Sidi 1997), they can be classified into three models: impulsive thrust model, infinite thrust model and low thrust model. According to whether or not the initial and final orbits have a common point, orbital maneuvering can be divided into different cases including orbital change, orbital transfer, etc. However, each type of maneuver will induce a maneuver velocity vector that consists of the radial, in-track and cross-track (RIC) components. In order to conveniently describe the state of an object's movement, the observations can be transformed into a full 6-parameter vector or a partial parameter vector of orbital elements based on different space surveillance systems and the formats of observations. Note also that none of the algorithms can be adapted to all possible scenarios and observations. In this paper, we focus on a well known situation (Sidi 1997; Kelecy & Jah 2010), where none or only one in-track orbital maneuver occurs during the time intervals between the different observations for a single orbital object. The observations are characterized by two groups of full 6-parameter vectors of orbital elements to illustrate the uncertainties. In this work, we propose a novel approach to achieve maneuver detection and object correlation, which can also be applied to other potential scenarios.

This paper is organized as follows. The observations and a model of orbital movement are introduced in Section 2. In Section 3, the posterior probabilities of orbital maneuver and a joint association event of space objects are analyzed based on the Joint Probabilistic Data Association (JPDA) algorithm. To derive the maximum posterior probability, the crucial step is the accurate reconstruction of the orbital maneuver time and velocity during the time intervals between the different observations. In this work, a novel approach is proposed in Section 4 for the detection and reconstruction

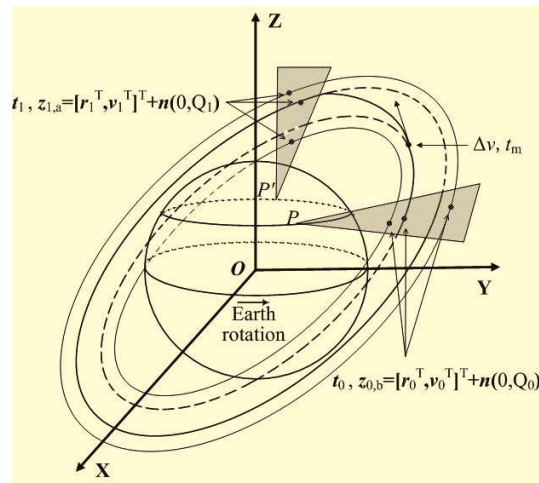


Fig. 1 The space surveillance scenario in the ECI coordinate frame.

of the orbital maneuver based on a constrained nonlinear least squares scheme. The performance of maneuver detection is also theoretically analyzed. Based on the maximum a posteriori (MAP) criterion, the desired decision and the corresponding confidence levels for object correlation and maneuver detection are presented in Section 5. The effectiveness and advantages of the proposed approach are validated through the simulation results in Sections 4 and 5. Section 6 concludes this work and addresses some open problems.

2 OBSERVATIONS AND MOVEMENT MODEL OF AN ORBITAL OBJECT

The orbital elements of space objects are important for identifying the targets and cataloging orbital objects when conducting space surveillance. This information is often obtained via observing several sections of an arc in the object's orbit through various observation devices, e.g. radar, optical telescope, etc. A diagram showing how the objects being observed are configured is illustrated in Figure 1.

In this paper, we assume that a full 6-parameter vector z of an orbital element can be provided from the observation, which consists of the position vector r and the velocity vector v in the Earth-centered inertial (ECI) coordinate frame at a certain time. We detect the maneuvers and finalize the correlations for the previously uncorrelated tracks between two arbitrarily observed periods. Each period may contain many different observation times. For convenience, the observed orbital elements at different times of a period are propagated to the same time. The observation time and the corresponding observations during the pre-period are denoted by t_0 and $z_{0,b}$, respectively. Those during the post-period are denoted by t_1 , and $z_{1,a}$. Δv and t_m are the in-track maneuvering velocity and maneuvering time of an orbiting object, respectively. O is the geocenter. P and P' are the positions of the observation station at times t_0 and t_1 , respectively.

By solving the Kepler problem without considering the perturbation force, we can describe the orbital movement using an elegant state transition matrix (Der 1997)

$$\begin{bmatrix} r_1 \\ v_1 \end{bmatrix} = \begin{bmatrix} fI & gI \\ \dot{f}I & \dot{g}I \end{bmatrix} \begin{bmatrix} r_0 \\ v_0 \end{bmatrix}. \quad (1)$$

In the ECI coordinate frame, r_0 , v_0 and r_1 , v_1 are the position vector and velocity vector of the object in space at times t_0 and t_1 , respectively. I is a unit matrix. f , g , \dot{f} and \dot{g} are functions of r_0 ,

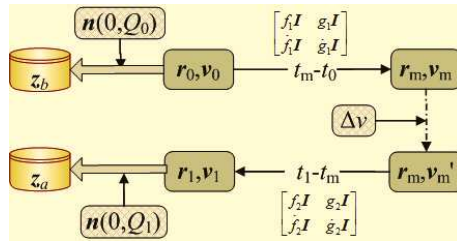


Fig. 2 The orbital maneuver process.

v_0 and $t_1 - t_0$. The concrete expression can be referred to in Der (1997). Equation (1) describes the non-maneuvering model of the object in space.

Any orbital maneuver is accompanied by a change in the velocity of the satellite, which consumes a certain quantity of fuel. For an orbital maneuver, minimization of fuel consumption is essential because the weight of a payload that can be carried to the desired orbit depends on this minimization. Therefore, choices in the modes of orbital maneuver are limited. The thrust imposed on the in-track direction is an efficient maneuvering mode for minimizing fuel consumption, which is commonly applied in the process of various orbital maneuvers (Sidi 1997; Kelecyc & Jah 2010). In addition, because the duration of thrust is almost instantaneous relative to the large gap between observations, the process of orbital maneuver can equivalently be considered as a single in-track impulsive thrust.

The process of orbital maneuver can be divided into two stages, as illustrated in Figure 2.

In Figure 2, r_m is the position vector at maneuver time t_m . v_m and v'_m are the pre-maneuver velocity vector and the post-maneuver velocity vector at time t_m , respectively. The orbit maneuvers are along the in-track direction, so we can derive $v'_m = v_m + \Delta v \cdot v_m / v_m$, where $v_m = \|v_m\|_2$, $\|\cdot\|_2$ denotes the ℓ_2 -norm. r_0, v_0 and r_1, v_1 are the position vector and velocity vector of space object at times t_0 and t_1 , respectively. f_1, g_1, \dot{f}_1 and \dot{g}_1 are functions of r_0, v_0 and $t_m - t_0$. f_2, g_2 and \dot{f}_2, \dot{g}_2 are functions of r_m, v'_m and $t_1 - t_m$. Assuming that the observations have Gaussian white noise with zero mean, $n(0, Q_0)$ and $n(0, Q_1)$ denote the observation noises at times t_0 and t_1 , respectively, where Q_0 and Q_1 are the noise covariance. Let $Q_0 = Q_1 = \text{diag}[\sigma_r^2, \sigma_r^2, \sigma_r^2, \sigma_v^2, \sigma_v^2, \sigma_v^2]$ in this paper. Thus, the observed orbital elements in the presence of noise are denoted by $z_{0,b} = [r_0^T, v_0^T]^T + n(0, Q_0)$ and $z_{1,a} = [r_1^T, v_1^T]^T + n(0, Q_1)$.

The orbital maneuvering model can be represented by the following equation:

$$\begin{cases} \begin{bmatrix} r'_1 \\ v'_1 \end{bmatrix} = \begin{bmatrix} r_1 \\ v_1 \end{bmatrix} + n(0, Q_1) \\ = \begin{bmatrix} f_2 I & g_2 I \\ \dot{f}_2 I & \dot{g}_2 I \end{bmatrix} \left(\begin{bmatrix} f_1 I & g_1 I \\ \dot{f}_1 I & \dot{g}_1 I \end{bmatrix} \begin{bmatrix} r_0 \\ v_0 \end{bmatrix} + \begin{bmatrix} 0 \\ \Delta v \cdot v_m / v_m \end{bmatrix} \right) + n(0, Q_1), \\ \begin{bmatrix} r'_0 \\ v'_0 \end{bmatrix} = \begin{bmatrix} r_0 \\ v_0 \end{bmatrix} + n(0, Q_0), \end{cases} \quad (2)$$

where $\begin{bmatrix} r_m \\ v_m \end{bmatrix} = \begin{bmatrix} f_1 I & g_1 I \\ \dot{f}_1 I & \dot{g}_1 I \end{bmatrix} \begin{bmatrix} r_0 \\ v_0 \end{bmatrix}$. If the orbital perturbation is taken into account, we should add the corresponding perturbing terms to Equation (2). However, when the effect of the perturbation force is uncorrelated with the orbital maneuvering parameters, the problem can be solved using the

same method whether or not it has a perturbation. For convenience, this paper does not consider the perturbation during the movement of an object in space.

3 PRINCIPLE OF MANEUVER DETECTION AND OBJECT CORRELATION

In Equation (2), the maneuvering time and velocity are unknown, which makes it possible that one observed orbit at time t_0 can create multiple potential orbits at time t_1 via a single in-track maneuver. Therefore, orbital maneuver and object correlation are feasible between two arbitrarily observed orbits. To solve the aforementioned problem of object correlation and maneuver detection of the uncorrelated tracks, the multiple hypothesis testing (MHT) method is a reasonable and well-known solution (Benoudnine et al. 2012). Let $\mathbf{Z} = \{\mathbf{Z}_0, \mathbf{Z}_1\}$ denote the observed orbital elements, where $\mathbf{Z}_0 = \{z_{0,1}, z_{0,2}, \dots, z_{0,b}, \dots, z_{0,B}\}$ and $\mathbf{Z}_1 = \{z_{1,1}, z_{1,2}, \dots, z_{1,a}, \dots, z_{1,A}\}$ are the observed orbital elements at times t_0 and t_1 , respectively. To simplify our presentation, we use b and a to denote the corresponding indexes for the numbers of the observed orbits in \mathbf{Z}_0 and \mathbf{Z}_1 . Similarly, B and A indicate the maximal ones observed at the different times mentioned above. All the feasible joint association events are denoted by $\theta = [\theta_i]$, $i = 1, 2, \dots, n$, and the corresponding validation matrix of the joint association event θ_i is (Fortmann et al. 1983)

$$\Omega(\theta_i) = [\omega_{ab}^i(\theta_i)] = \begin{bmatrix} \omega_{10}^i & \cdots & \omega_{1B}^i \\ \vdots & \ddots & \vdots \\ \omega_{A0}^i & \cdots & \omega_{AB}^i \end{bmatrix}, \quad (3)$$

where $\omega_{ab}^i(\theta_i)$ is a binary variable. $\omega_{ab}^i = 1$ indicates that the observed orbit $z_{1,a}$ at time t_1 is correlated with the observed orbit $z_{0,b}$ at time t_0 , and $\omega_{ab}^i = 0$ indicates that they are uncorrelated. $b = 0$ represents a newly observed object (new object and false alarm are considered as the same event in this paper). According to the rule for constructing joint association events (Fortmann et al. 1983),

the validation matrix should satisfy $\sum_{b=0}^B \omega_{ab}^i = 1$, $a = 1, 2, \dots, A$; $\sum_{a=1}^A \omega_{ab}^i \leq 1$, $b = 1, 2, \dots, B$.

In the same way, the validation matrix for maneuvering is defined as M^i under the feasible joint association event θ_i . Thus, all the possible maneuvering events are $\mathbf{M} = [M^i]$, $i = 1, 2, \dots, n$. The concrete form of the validation matrix for maneuvering is

$$M^i = [m_{ab}^i(\theta_i)] = \begin{bmatrix} m_{10}\omega_{10}^i & \cdots & m_{1B}\omega_{1B}^i \\ \vdots & \ddots & \vdots \\ m_{A0}\omega_{A0}^i & \cdots & m_{AB}\omega_{AB}^i \end{bmatrix}, \quad (4)$$

where m_{ab} is also a binary variable with $m_{ab} = 1$ indicating that the orbital maneuver occurs when a space object moves from the observed orbit $z_{0,b}$ to $z_{1,a}$, and $m_{ab} = 0$ indicates that there is no orbital maneuver. Assuming that the orbital maneuver does not occur for the newly observed object, the value of element m_{a0} in the matrix M is zero. $m_{ab}^i = m_{ab}\omega_{ab}^i$ suggests that the maneuver event is only detected in the case that the orbits a and b are hypothetically correlated.

The essence of maneuver detection and object correlation is to reconstruct the orbital maneuver parameters over the large observation gaps and obtain the MAP estimation of a joint association event based on two groups of observed orbital elements in the presence of observational uncertainty, i.e.

$$[\theta_i, M^i] = \arg \max_{\theta} \left(\arg \max_{\mathbf{M}} p(\mathbf{M}, \theta | \mathbf{Z}) \right). \quad (5)$$

The posterior probability in Equation (5) can be evaluated using the Bayesian formula

$$p(M^i, \theta_i | \mathbf{Z}) = \frac{p(\mathbf{Z} | M^i, \theta_i) p(M^i | \theta_i) p(\theta_i)}{p(\mathbf{Z})}, \quad (6)$$

where the posterior probability approximately represents the confidence of the decision.

We can incorporate two binary indicators given by

$$\tau_a(\theta_i) = \sum_{b=1}^B \omega_{ab}^i(\theta_i) = \begin{cases} 1 \\ 0 \end{cases}, \quad (7)$$

which indicates whether or not the observed orbit a at time t_1 is correlated with an observed orbit at time t_0 .

$$\delta_b(\theta_i) = \sum_{a=1}^A \omega_{ab}^i(\theta_i) = \begin{cases} 1 \\ 0 \end{cases}, \quad (8)$$

which indicates whether or not the observed orbit b at time t_0 is correlated with an observed orbit at time t_1 . Let $\phi(\theta_i)$ denote the number of newly observed objects in the joint association event θ_i .

Thus, we can obtain $\phi(\theta_i) = \sum_{a=1}^A [1 - \tau_a(\theta_i)]$.

In many radar applications, the JPDA algorithm provides a reliable performance about data association in dense multiple target environments and is very robust with respect to the real-world environment (Bar-Shalom et al. 2009). According to the parametric JPDA algorithm, the evaluation of posterior probability for a joint event is done as follows (Bar-Shalom et al. 2009):

$$\begin{aligned} p(M^i, \theta_i | \mathbf{Z}) &= \frac{\lambda^{\phi(\theta_i)}}{c'} \prod_{a=1}^A \prod_{b=1}^B \{ \max P(m_{ab}^i(\theta_i) | \mathbf{z}_{1,a}, \mathbf{z}_{0,b}) \}^{\omega_{ab}^i(\theta_i)} \prod_{b=1}^B (P_D^b)^{\delta_b(\theta_i)} (1 - P_D^b)^{1 - \delta_b(\theta_i)} \\ &= \frac{\lambda^{\phi(\theta_i)}}{c} \prod_{a=1}^A \prod_{b=1}^B \{ \max N[\mathbf{z}_{1,a}; \hat{\mathbf{z}}_{ab} | \mathbf{z}_{0,b}, \mathbf{S}_{ab}, m_{ab}^i(\theta_i)] P[m_{ab}^i(\theta_i)] \}^{\omega_{ab}^i(\theta_i)} \\ &\quad \cdot \prod_{b=1}^B (P_D^b)^{\delta_b(\theta_i)} (1 - P_D^b)^{1 - \delta_b(\theta_i)}, \end{aligned} \quad (9)$$

where λ is the spatial density of the newly observed objects, P_D^b is the detection probability of the orbit b at time t_1 , and c' and c are the normalization parameters. Assuming the correlation of orbit a with orbit b has a Gaussian probability distribution, let $N[\mathbf{z}_{1,a}; \hat{\mathbf{z}}_{ab} | \mathbf{z}_{0,b}, \mathbf{S}_{ab}, m_{ab}^i(\theta_i)]$ be the conditional probability of the correlation under a certain model of maneuvering (i.e. $m_{ab}^i(\theta_i) = 0$ or 1), $\hat{\mathbf{z}}_{ab} | \mathbf{z}_{0,b}$ is orbit b 's predicted orbit at time t_1 in the maneuver model $m_{ab}^i(\theta_i)$, and \mathbf{S}_{ab} is the corresponding covariance of the predicted orbit. $P[m_{ab}^i(\theta_i)]$ is the prior probability of the orbital maneuver model. In practical application, we can obtain prior knowledge of $P[m_{ab}^i(\theta_i) = 1] / P[m_{ab}^i(\theta_i) = 0] = \Lambda$ from the statistical probability of maneuvering events of all cataloged space objects for different gaps of the observations. Λ is a small value in the current space environment. In addition, based on our experiments, the result is not very sensitive to Λ when its value is smaller than 0.001.

In order to obtain the MAP estimation, there are two main problems that need to be solved: firstly, in the case of a joint event θ_i , we must obtain the validation matrix of the maneuver M^i by maximizing the posterior probability of $P(m_{ab}^i(\theta_i) | \mathbf{z}_{1,a}, \mathbf{z}_{0,b})$, which is named maneuver detection; secondly, calculate $p(M^i, \theta_i | \mathbf{Z})$ for all the feasible joint association events $\theta = [\theta_i], i = 1, 2, \dots, n$, and select the validation matrix which has the maximum value of $p(M^i, \theta_i | \mathbf{Z})$ as the final estimated result, which is named the MAP evaluation.

4 ORBITAL MANEUVER DETECTION

In the case of a joint association event θ_i , a Bayesian decision is applied to test for a correlation in the maneuver event for the hypothetical pair of orbits a and b

$$\begin{aligned} \text{if} \quad & \max P(m_{ab}^i(\theta_i) = 1 | \mathbf{z}_{1,a}, \mathbf{z}_{0,b}) \geq \max P(m_{ab}^i(\theta_i) = 0 | \mathbf{z}_{1,a}, \mathbf{z}_{0,b}) \\ \text{decision} \quad & m_{ab}^i(\theta_i) = \begin{cases} 1 \\ 0 \end{cases}, \end{aligned} \quad (10)$$

where

$$\begin{aligned} \max P(m_{ab}^i(\theta_i) | \mathbf{z}_{1,a}, \mathbf{z}_{0,b}) &= \max c'' N[\mathbf{z}_{1,a}; \hat{\mathbf{z}}_{ab} | \mathbf{z}_{0,b}, \mathbf{S}_{ab}, m_{ab}^i(\theta_i)] P[m_{ab}^i(\theta_i)] \\ &= \max c'' \frac{1}{\sqrt{2\pi |\mathbf{S}_{ab}|}} \exp\left[(\mathbf{z}_{1,a} - \hat{\mathbf{z}}_{ab} | \mathbf{z}_{0,b})^T \mathbf{S}_{ab}^{-1} (\mathbf{z}_{1,a} - \hat{\mathbf{z}}_{ab} | \mathbf{z}_{0,b})\right] P[m_{ab}^i(\theta_i)], \end{aligned} \quad (11)$$

where c'' is a normalization parameter. When $m_{ab}^i(\theta_i) = 0$, the maximum posterior probability in the non-maneuvering mode can be calculated directly. However, when $m_{ab}^i(\theta_i) = 1$, the unknown parameters of maneuver time and velocity must first be estimated. Assuming that a single in-track maneuver velocity Δv is applied to the space object at time t_m ($t_0 \leq t_m \leq t_1$), a simplified equivalent least squares estimation is used to substitute the MAP estimation problem in Equation (11)

$$\begin{aligned} & \arg \min_{\Delta v, t_m} (\mathbf{z}_{1,a} - \hat{\mathbf{z}}_{ab} | \mathbf{z}_{0,b})^T Q_1^{-1} (\mathbf{z}_{1,a} - \hat{\mathbf{z}}_{ab} | \mathbf{z}_{0,b}) \\ & \approx \arg \max_{\Delta v, t_m} N[\mathbf{z}_{1,a}; \hat{\mathbf{z}}_{ab} | \mathbf{z}_{0,b}, \mathbf{S}_{ab}, m_{ab}^i(\theta_i)]. \end{aligned} \quad (12)$$

4.1 Method of Parameter Estimation in Orbital Maneuvering

The first equation in the maneuvering model of Equation (2) is abbreviated as

$$\begin{bmatrix} \mathbf{r}'_1{}^T \\ \mathbf{v}'_1{}^T \end{bmatrix}^T = \Phi(\mathbf{r}_0, \mathbf{v}_0, \Delta v, t_m) + \mathbf{n}(0, Q_1).$$

Substituting it into the objective function of the least squares problem in Equation (12), we can obtain

$$\begin{bmatrix} \Delta \hat{v} \\ \hat{t}_m \end{bmatrix} = \arg \min_{\Delta v, t_m} \left(\begin{bmatrix} \mathbf{r}'_1 \\ \mathbf{v}'_1 \end{bmatrix} - \Phi(\mathbf{r}_0, \mathbf{v}_0, \Delta v, t_m) \right)^T Q_1^{-1} \left(\begin{bmatrix} \mathbf{r}'_1 \\ \mathbf{v}'_1 \end{bmatrix} - \Phi(\mathbf{r}_0, \mathbf{v}_0, \Delta v, t_m) \right). \quad (13)$$

Equation (13) is a non-linear least squares problem, with unknown parameter vector $\xi = [\mathbf{r}_0, \mathbf{v}_0, \Delta v, t_m]^T$. Before the Gauss-Newton iterative algorithm is applied, we need to compute the linearized form of $\Phi(\mathbf{r}_0, \mathbf{v}_0, \Delta v, t_m)$ at the parameter vector ξ (Storch 2005)

$$\mathbf{H}(\xi) = [\mathbf{H}(\mathbf{r}_0), \mathbf{H}(\mathbf{v}_0), \mathbf{H}(\Delta v), \mathbf{H}(t_m)] = \left[\frac{\partial \Phi}{\partial \mathbf{r}_0}, \frac{\partial \Phi}{\partial \mathbf{v}_0}, \frac{\partial \Phi}{\partial \Delta v}, \frac{\partial \Phi}{\partial t_m} \right]. \quad (14)$$

The partial derivatives are calculated in Appendix A.

The initial value $\xi(0)$ of the parameter vector ξ directly affects the convergence of the iterative algorithm. It is important to choose an appropriate initial value based on the prior information of the correlated orbits. In this paper, the observed values of \mathbf{r}'_0 and \mathbf{v}'_0 at time t_0 can be taken as the initial values of \mathbf{r}_0 and \mathbf{v}_0 . Moreover, let the observed orbits a and b propagate in the time interval $[t_0, t_1]$. We calculate the intersection time t'_m when the two orbits show the minimum difference in the magnitude of their position vectors through cross propagation. Thus, t'_m is chosen as the

initial iterative value of t_m , and the corresponding magnitude value $\Delta v'$ of the two velocity vectors' difference at the intersection point is chosen as the initial value of maneuvering velocity Δv .

In order to obtain a more sensible and accurate result, the constraints for the unknown parameter vector ξ should be applied in the iteration process. The constrained iterative form used for solving the non-linear least squares problem is:

$$\begin{aligned} \xi(n+1) &= \arg \min_{\hat{\xi}(n+1)} \left(\begin{bmatrix} r'_1 \\ v'_1 \end{bmatrix} - \Phi(\xi(n)) + H(\xi(n)) [\xi(n) - \hat{\xi}(n+1)] \right)^T \\ &\cdot Q_1^{-1} \left(\begin{bmatrix} r'_1 \\ v'_1 \end{bmatrix} - \Phi(\xi(n)) + H(\xi(n)) [\xi(n) - \hat{\xi}(n+1)] \right), \\ \text{s.t.} \quad &\begin{cases} \left\| \begin{bmatrix} r_0(n+1) \\ v_0(n+1) \end{bmatrix} - \begin{bmatrix} r'_0 \\ v'_0 \end{bmatrix} \right\|_2 \leq \begin{bmatrix} 3\sigma_r \mathbf{1}_3 \\ 3\sigma_v \mathbf{1}_3 \end{bmatrix} \\ 0 \leq \Delta v(n+1) \leq \Delta v_{\max} \\ t_0 \leq t_m(n+1) \leq t_1 \end{cases}, \end{aligned} \quad (15)$$

where Δv_{\max} is the upper bound of the maneuvering velocity. The iterative process is an optimization problem, which can be handled by the SOCP algorithm (Lobo et al. 1998). Therefore, the maneuvering time \hat{t}_m and the maneuvering velocity $\Delta \hat{v}$ can be estimated by multiple iterations.

4.2 Detection Performance of Orbital Maneuver

Let $\mathbf{x} = [r_1^T, v_1^T, r_0^T, v_0^T]^T$ be the observations. Using the parameter vector $\xi = [r_0, v_0, \Delta v, t_m]^T$, we can calculate the mathematical expectation of the observations $\mu(\xi) = [r_1^T, v_1^T, r_0^T, v_0^T]^T = [\Phi(\xi)^T, r_0^T, v_0^T]^T$. The observation covariance is $Q = \text{diag}[Q_1, Q_0]$ and the probability density function of the observations is

$$p(\mathbf{x}; \xi) = \frac{1}{(2\pi)^6 |Q|} \exp \left[-\frac{1}{2} (\mathbf{x} - \mu(\xi))^T Q^{-1} (\mathbf{x} - \mu(\xi)) \right]. \quad (16)$$

Therefore, the element in the Fisher information matrix for the unknown parameters is

$$[\mathbf{I}(\xi)]_{kl} = \frac{\partial \mu(\xi)^T}{\partial \xi_k} Q^{-1} \frac{\partial \mu(\xi)}{\partial \xi_l}. \quad (17)$$

Using Equation (14), $\partial r_0 / \partial \xi$ and $\partial v_0 / \partial \xi$, we can easily obtain the Cramer-Rao lower bound (CRLB) of the estimated parameters t_m and Δv . Here, two common gaps of the observations are used for analyzing the performance, i.e. one case is that the surveillance system observes two adjacent orbits of an object, whose time interval is about an orbital period (about two hours for an object in low Earth orbit); the other case is when an ascending arc and a descending arc of the same orbit are observed, whose time interval is about 12 hours. In this paper, the parameters for the simulation are set as follows: the initial orbit elements are semi-major axis $a = 7000$ km, eccentricity $e = 0.01$, inclination $i = 70^\circ$, longitude of the ascending node $\Omega = 170^\circ$, argument of periapsis $\omega = 30^\circ$, mean anomaly $M = 30^\circ$; the observation errors are $\sigma_r = 10$ m and $\sigma_v = 0.1$ m s⁻¹. Subsequently, we calculate the CRLBs in the simulation. For the non-maneuvering object, the CRLB's square root of the maneuvering velocity is 0.1 m s⁻¹, which is similar to the observation error. For the maneuvering objects, the distributions of the CRLBs' square root of the estimated maneuvering time and velocity are shown in Figure 3.

Figure 3 indicates that the precision of estimation fluctuates with respect to the maneuvering time instead of changing monotonically. With the increase of maneuvering velocity, the parameters

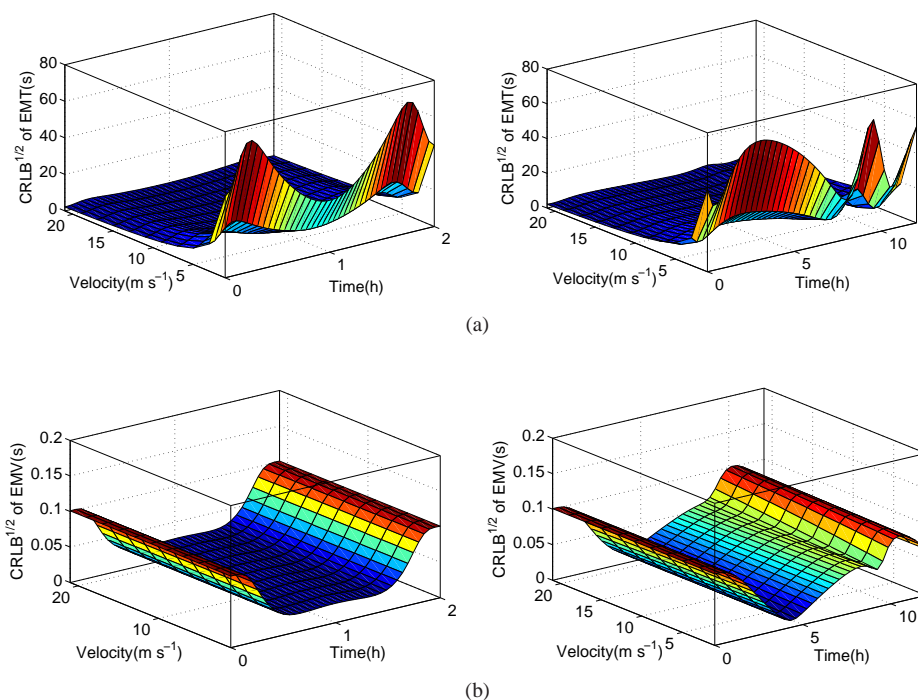


Fig. 3 The distribution of the CRLBs' square root of the estimated maneuvering time (a) and velocity (b).

Table 1 Cumulative Probability Distribution of the Estimated Maneuver Velocity for the Non-maneuvering Object

Estimated maneuvering velocity (m s ⁻¹)	$\leq 10^{-3}$	$\leq 10^{-2}$	≤ 0.1	≤ 0.3	≤ 0.6
Cumulative probability (2 hours)	0.4500	0.4550	0.6500	0.9450	1
Cumulative probability (12 hours)	0.5050	0.5250	0.7000	0.9950	1

will be estimated with a higher precision. In addition, the precision of estimation for a large gap $t_1 - t_0$ in observations is slightly higher than that for a small one.

Furthermore, Monte Carlo simulations are carried out to examine and analyze the performance of maneuver detection and precision of parameter estimation in the proposed algorithm. The result is compared with the CRLB. The parameters in the simulation are the same as the aforementioned settings.

Firstly, we carry out the maneuver detection for the non-maneuvering object. The cumulative probability distribution of the estimated maneuvering velocity is shown in Table 1.

Table 1 indicates that almost all the estimated maneuvering velocities are less than $3\sigma_v$, which results from observation errors. In other words, there is quite a small probability that a non-maneuvering object would be identified as a maneuvering one.

Subsequently, the maneuver detection is carried out for the maneuvering object. In this paper, when the estimation biases satisfy $\delta(t_m) \leq 60$ s and $\delta(\Delta v) \leq 0.3$ m s⁻¹, we assume that the orbital maneuver detection is correct. Only the correct maneuver detection is used to evaluate the accuracy of the parameter estimation. The result is shown in Figure 4.

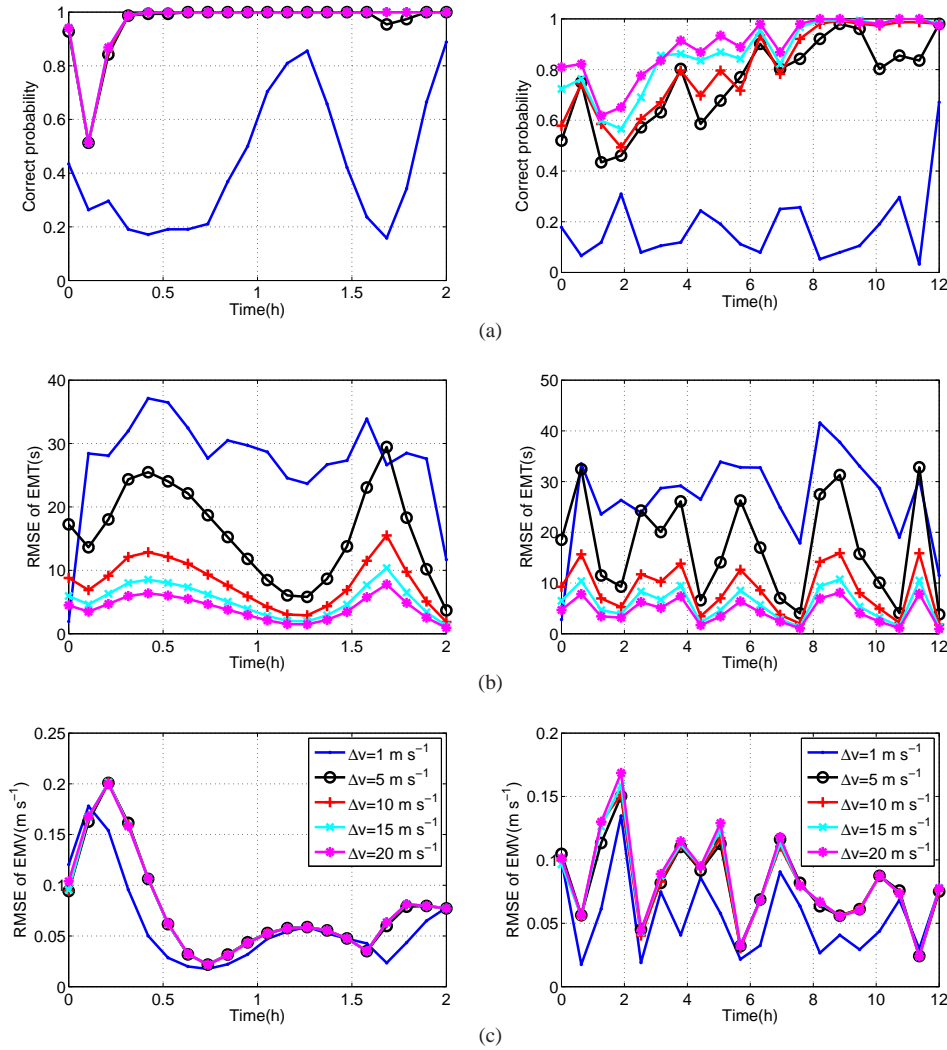


Fig. 4 The performance of the proposed maneuver detection algorithm. (a) Probability of correct maneuver detection, (b) Root Mean Square Error (RMSE) of the estimated maneuver time, (c) Root Mean Square Error (RMSE) of the estimated maneuver velocity.

Figure 4 suggests that the detection performance is closely related with the real maneuver time and the maneuver velocity. Comparing the simulation results with the CRLBs, we can find that it will acquire a high probability of correct detection where the CRLBs of the maneuver time and velocity are low. When the maneuver velocity exceeds 5 m s^{-1} , the probability of correct maneuver detection probability can be as high as 1. With increasing maneuver velocity, the estimated accuracy of the maneuver time is improved. However, the estimated accuracy of the maneuver velocity is more sensitive to the real maneuver time, which coincides with the trend of the CRLB. In addition, Figure 4 also shows that a larger gap interval of the observations leads to a higher estimated accuracy than a smaller one, but the probability of correct detection is much lower. The reasons behind this

outcome are that it is much more difficult to get an accurate initial value for the iteration for the case of a large gap interval than for a small gap. The larger difference between the initial iterative value and the real value will result in a higher probability of non-convergence as well as a problem with local convergence. This is the main reason why a larger gap of observations makes the detection of an orbital maneuver more difficult.

5 OBJECT CORRELATION BASED ON THE MAP CRITERION

5.1 Evaluation of the Maximum Posterior Probability

According to the results of the maneuver detection, the maneuver time \hat{t}_m and the maneuver velocity $\Delta\hat{v}$ are estimated in the maneuver mode. Substituting the observed orbit b and the maneuver parameters into the maneuver model, we can calculate $\hat{z}_{ab}|z_{0,b}$. Assuming that the prediction errors are independent in all the dimensions, i.e. the covariance matrix \mathbf{S}_{ab} is diagonal, the square roots of the diagonal elements are

$$\begin{bmatrix} \delta r_1 \\ \delta v_1 \end{bmatrix} = \mathbf{H}(\boldsymbol{\xi}) \begin{bmatrix} \delta r_0^T & \delta v_0^T & \delta\Delta\hat{v} & \delta\hat{t}_m \end{bmatrix}^T, \quad (18)$$

where $\delta\Delta\hat{v} = \sqrt{\text{CRLB}(\Delta\hat{v})}$ and $\delta\hat{t}_m = \sqrt{\text{CRLB}(\hat{t}_m)}$. The correlation probability $N[z_a; \hat{z}_{ab}|z_b, \mathbf{S}_{ab}, m_{ab}^i(\theta_i) = 1]$ in the maneuvering mode can be calculated based on Equation (11). For the non-maneuvering mode, $\hat{z}_{ab}|z_b$ can be obtained from the state transition matrix. The square roots of the diagonal elements in the covariance matrix \mathbf{S}_{ab} are calculated by

$$\begin{bmatrix} \delta r_1 \\ \delta v_1 \end{bmatrix} = \begin{bmatrix} \tilde{\mathbf{R}}(t) & \mathbf{R}(t) \\ \tilde{\mathbf{V}}(t) & \mathbf{V}(t) \end{bmatrix} \begin{bmatrix} \delta r_0 \\ \delta v_0 \end{bmatrix}. \quad (19)$$

Therefore, the correlation probability $N[z_{1,a}; \hat{z}_{ab}|z_{0,b}, \mathbf{S}_{ab}, m_{ab}^i(\theta_i) = 0]$ for the non-maneuvering mode can be calculated. Accordingly, the posterior probability $p(M^i, \theta_i | \mathbf{Z})$ of the joint association event θ_i and the corresponding validation matrix for maneuvering M^i can easily be obtained. The joint association event and the orbital maneuver are then estimated and detected based on the MAP decision.

5.2 Performance Analysis of Object Correlation

In order to validate the effectiveness of the proposed algorithm, a simulated scenario is presented where the incorrect correlations are most likely to take place. Consider two coplanar orbits: one is an orbit through a single in-track maneuver; the other is a non-maneuvering orbit. The main reason for the incorrect correlation is that the observed orbits are very close to each other at the pre-maneuver observation time t_0 or the post-maneuver observation time t_1 . These two scenarios are completely symmetric, so the performances of object correlation are the same. In this paper, we analyze the performance using the scenario that the observed orbits are very close to each other at the pre-maneuver observation time t_0 , which is illustrated in Figure 5.

When the orbits are coplanar, the difference in orbital altitude is commonly used to describe the degree of closeness of the two orbits while the other orbital elements keep the same values. In the presence of observational uncertainty, we adjust the interval of orbital altitude between the two orbits for analyzing the correlation performance. The orbital element and the observation error are the same as the parameter setting in the simulation of maneuver detection. The orbit maneuver occurs at the center of the observations' interval. In the simulation, the orbital altitude interval increases with a step of 25 m, and the prior probability of the orbital maneuver is set to $\Lambda = 0.001$. The probability P_d of the correct object correlation as well as the correct maneuver detection and the mean value of the corresponding maximum posterior probability are shown in Figure 6.

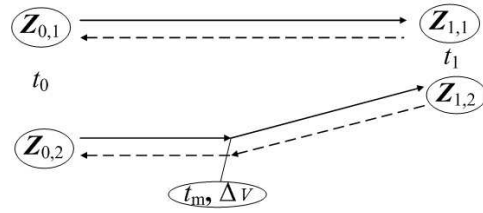


Fig. 5 The scenario for the performance analysis of object correlation.

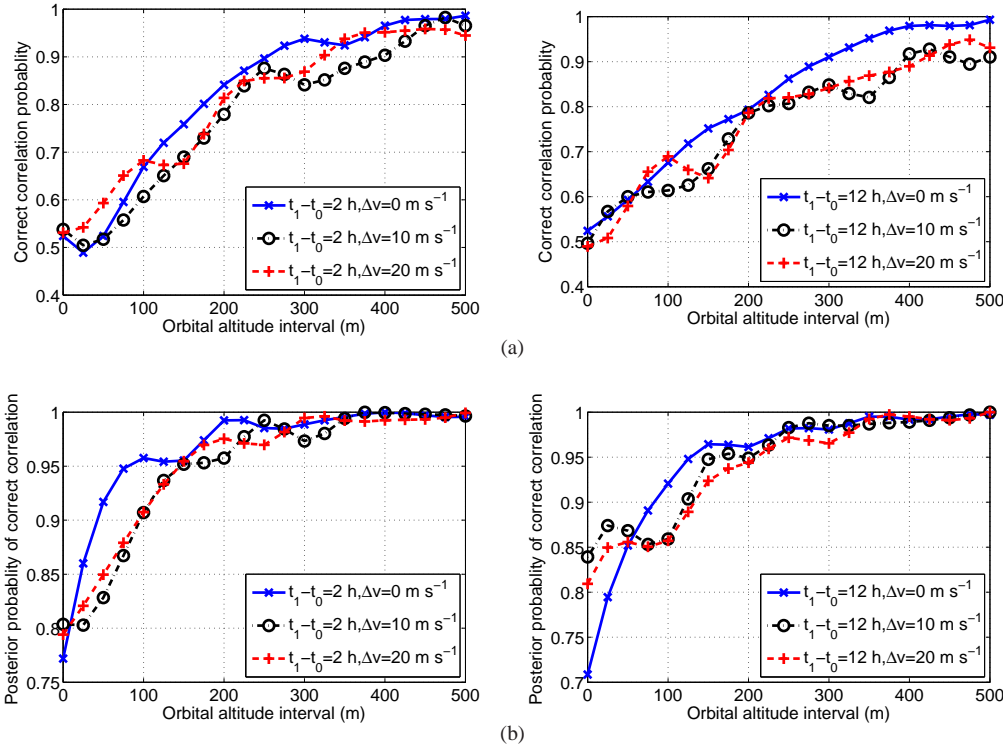


Fig. 6 Correct correlation probability and the corresponding posterior probability vs. the orbital altitude interval. (a) Correct correlation probability vs. the orbital altitude interval. (b) The corresponding posterior probability of correct object correlation.

Figure 6 suggests that the ratio of correct object correlation increases as the interval of orbits' altitude becomes larger. When the orbital altitude interval is 500 m, the correct correlation probability approaches 0.95, and the corresponding maximum posterior probability (confidence value) tends to 1. Furthermore, we can see that it achieves the highest correct correlation probability and confidence value for the non-maneuvering object and also a larger maneuver velocity can attain higher performance and reliability than a smaller one. In addition, the larger gap of the observation will slightly decrease the performance of the correct object correlation. Generally speaking, the performance of

the proposed algorithm is related to many factors, including the gaps of the observations, the maneuver time, and the maneuver velocity. The success of object correlation is largely dependent on correct maneuver detection.

6 CONCLUSIONS AND FUTURE WORK

Maneuver detection and object correlation for uncorrelated tracks play an important role in space surveillance. This paper presents a novel method to address the problem of object correlation of uncorrelated tracks with a single in-track orbital maneuver. We accurately estimate the maneuvering time and velocity by solving a constrained non-linear least squares iterative problem using the SOCP algorithm. Subsequently, according to the JPDA algorithm, the posterior probability of the feasible joint association event and validation matrix for the maneuver are evaluated. Finally, the MAP decision is used to optimally find object correlation and maneuver detection. The performance of the proposed method is also analyzed in detail, and extensive simulations are carried out to validate the effectiveness of the algorithm.

This paper mainly focuses on the problem of object correlation and maneuver detection in a special situation, where we only consider a single in-track orbital maneuver during observation gaps, and the perturbation is not taken into account. However, the proposed algorithm is a general methodology, which can be adapted to many different situations. A more complex situation will be handled in future work. The following typical cases are given as examples.

Case 1: consider the perturbation. Generally speaking, the values of the partial derivative of the perturbation force at the maneuver time and velocity are not very large. Therefore, by implementing the numerical integration of the perturbation force into the iterative process of the maneuver detection, the algorithm can be applied to solve the problem with a perturbation.

Case 2: non-in-track maneuver. If the object maneuvers not only in the in-track direction, much more prior information about the orbital maneuver, such as the minimum energy principle (Holzinger & Scheeres 2010) and Q-law (Petropoulos 2005), should be explored to constrain the maneuvering model for estimating the optimum maneuver parameters. Based on the estimated maneuver parameters, we can evaluate the maximum posterior probability of object correlation and maneuver detection using the JPDA.

Case 3: multiple orbital maneuvers. When orbital maneuvering times are known, the single maneuver model can be extended to a more definitive model describing maneuvering times, and the proposed method can be applied to multiple orbital maneuvers in the same way. However, in the case of unknown times of orbital maneuver, the maneuver times must first be estimated. The orbital maneuvering times during the gap of the observations are usually sparse, so we can reconstruct the maneuver times based on some efficient algorithms such as sparse reconstruction (Figueiredo et al. 2007) or a global searching algorithm. Then the final results can be obtained using the aforementioned method.

Appendix A: CALCULATION OF THE LINEARIZED FORM OF THE TRANSITION MATRIX IN THE MANEUVER MODE

The following parameters can be derived from the definitions in Der (1997): during the period from time t_0 to the maneuver time t_m , parameters $\tilde{\mathbf{R}}_1(t)$, $\mathbf{R}_1(t)$, $\tilde{\mathbf{V}}_1(t)$, $\mathbf{V}_1(t)$, f_1 , g_1 , \dot{f}_1 and \dot{g}_1 are known and defined; during the period from the maneuver time t_m to the maneuver time t_1 , parameters α , f_2 , g_2 , \dot{f}_2 , \dot{g}_2 , A_1 , B_1 , A_2 , B_2 , A_3 , B_3 , \dot{A}_1 , \dot{A}_2 , \dot{A}_3 , \dot{B}_1 , \dot{B}_2 and \dot{B}_3 are already known and defined. $\mu = 3.98600436 \times 10^{14} \text{ m}^3 \text{ s}^{-2}$ is the Earth's gravitational constant.

Let $\Delta \mathbf{v}_m = \Delta v \cdot \mathbf{v}_m / v_m$, then we can obtain that

$$\begin{aligned} \mathbf{H}(\mathbf{r}_0) &= \begin{bmatrix} \partial f_2 / \partial \mathbf{r}_0 & \partial g_2 / \partial \mathbf{r}_0 \\ \partial \dot{f}_2 / \partial \mathbf{r}_0 & \partial \dot{g}_2 / \partial \mathbf{r}_0 \end{bmatrix} \begin{bmatrix} \mathbf{r}_m \\ \mathbf{v}_m \end{bmatrix} + \begin{bmatrix} f_2 \tilde{\mathbf{R}}_1(t) + g_2 \tilde{\mathbf{V}}_1(t) \\ \dot{f}_2 \tilde{\mathbf{R}}_1(t) + \dot{g}_2 \tilde{\mathbf{V}}_1(t) \end{bmatrix} \\ &+ \begin{bmatrix} \partial g_2 / \partial \mathbf{r}_0 \\ \partial \dot{g}_2 / \partial \mathbf{r}_0 \end{bmatrix} \Delta \mathbf{v}_m + \begin{bmatrix} g_2 \\ \dot{g}_2 \end{bmatrix} \frac{\partial \Delta \mathbf{v}_m}{\partial v_m} \tilde{\mathbf{V}}_1(t), \end{aligned} \quad (\text{A.1})$$

$$\begin{aligned} \mathbf{H}(\mathbf{v}_0) &= \begin{bmatrix} \partial f_2 / \partial \mathbf{v}_0 & \partial g_2 / \partial \mathbf{v}_0 \\ \partial \dot{f}_2 / \partial \mathbf{v}_0 & \partial \dot{g}_2 / \partial \mathbf{v}_0 \end{bmatrix} \begin{bmatrix} \mathbf{r}_m \\ \mathbf{v}_m \end{bmatrix} + \begin{bmatrix} f_2 \mathbf{R}_1(t) + g_2 \mathbf{V}_1(t) \\ \dot{f}_2 \mathbf{R}_1(t) + \dot{g}_2 \mathbf{V}_1(t) \end{bmatrix} \\ &+ \begin{bmatrix} \partial g_2 / \partial \mathbf{v}_0 \\ \partial \dot{g}_2 / \partial \mathbf{v}_0 \end{bmatrix} \Delta \mathbf{v}_m + \begin{bmatrix} g_2 \\ \dot{g}_2 \end{bmatrix} \frac{\partial \Delta \mathbf{v}_m}{\partial v_m} \mathbf{V}_1(t), \end{aligned} \quad (\text{A.2})$$

$$\mathbf{H}(\Delta v) = \begin{bmatrix} \partial f_2 / \partial \Delta v & \partial g_2 / \partial \Delta v \\ \partial \dot{f}_2 / \partial \Delta v & \partial \dot{g}_2 / \partial \Delta v \end{bmatrix} \begin{bmatrix} \mathbf{r}_m \\ \mathbf{v}_m \end{bmatrix} + \begin{bmatrix} \partial g_2 / \partial \Delta v \\ \partial \dot{g}_2 / \partial \Delta v \end{bmatrix} \Delta \mathbf{v}_m + \begin{bmatrix} g_2 \\ \dot{g}_2 \end{bmatrix} \frac{\partial \Delta \mathbf{v}_m}{\partial \Delta v}, \quad (\text{A.3})$$

$$\begin{aligned} \mathbf{H}(t_m) &= \begin{bmatrix} \partial f_2 / \partial t_m & \partial g_2 / \partial t_m \\ \partial \dot{f}_2 / \partial t_m & \partial \dot{g}_2 / \partial t_m \end{bmatrix} \begin{bmatrix} \mathbf{r}_m \\ \mathbf{v}_m \end{bmatrix} + \begin{bmatrix} f_2 & g_2 \\ \dot{f}_2 & \dot{g}_2 \end{bmatrix} \begin{bmatrix} \dot{f}_1 & \dot{g}_1 \\ \ddot{f}_1 & \ddot{g}_1 \end{bmatrix} \begin{bmatrix} \mathbf{r}_0 \\ \mathbf{v}_0 \end{bmatrix} \\ &+ \begin{bmatrix} \partial g_2 / \partial t_m \\ \partial \dot{g}_2 / \partial t_m \end{bmatrix} \Delta \mathbf{v}_m + \begin{bmatrix} g_2 \\ \dot{g}_2 \end{bmatrix} \frac{\partial \Delta \mathbf{v}_m}{\partial t_m}, \end{aligned} \quad (\text{A.4})$$

where $\frac{\partial \Delta \mathbf{v}_m}{\partial t_m} = -\frac{\Delta v \mu}{v_m r_m^3} \mathbf{r}_m - \frac{\mu \|\mathbf{r}_m\|_2}{r_m^3 v_m^3} \mathbf{v}_m$, $\frac{\partial \Delta \mathbf{v}_m}{\partial v_m} = \mathbf{I}_{3 \times 3} \frac{\Delta v}{v_m} + \frac{\Delta v}{v_m^3} \mathbf{v}_m \mathbf{1}_3^T$,

$$\ddot{f}_2 = -\frac{\mu}{r_1^3} \left(\frac{\|\mathbf{r}_1\|_2}{\|g_2/f_2 \mathbf{v}'_m + \mathbf{r}_m\|_2} \right), \quad \ddot{g}_2 = -\frac{\mu}{r_1^3} \left(\frac{\|\mathbf{r}_1\|_2}{\|f_2/g_2 \mathbf{r}_m + \mathbf{v}'_m\|_2} \right).$$

Other partial derivatives are calculated as follows:

$$\frac{\partial f_2}{\partial \Delta v} = F_1(A_1, A_3) = A_1 \frac{2}{\alpha \mu} v'_m + A_3 \frac{\mathbf{r}_m^T \mathbf{v}_m}{\sqrt{\mu v_m}}, \quad (\text{A.5})$$

$$\begin{aligned} \frac{\partial f_2}{\partial t_m} &= -\dot{f}_2 + F_2(A_1, A_2, A_3) = -\dot{f}_2 + \left(\frac{2A_1}{\alpha r_m^3} \mathbf{r}_m + \frac{A_2}{r_m} \mathbf{r}_m + \frac{A_3}{\sqrt{\mu}} \mathbf{v}'_m \right)^T \mathbf{v}_m \\ &+ \left(\frac{2A_1}{\alpha \mu} \mathbf{v}'_m + \frac{A_3}{\sqrt{\mu}} \mathbf{r}_m \right)^T \cdot \left(-\frac{\mu(1 + \Delta v)}{v_m r_m^3} \mathbf{r}_m - \frac{\mu \Delta v \|\mathbf{r}_m\|_2}{r_m^3 v_m^3} \mathbf{v}_m \right), \end{aligned} \quad (\text{A.6})$$

$$\begin{aligned} \frac{\partial f_2}{\partial \mathbf{r}_0} &= F_3(A_1, A_2, A_3) \\ &= \left(A_1 \frac{2}{\alpha r_m^3} \mathbf{r}_m + A_2 \frac{\mathbf{r}_m}{r_m} + A_3 \frac{\mathbf{v}'_m}{\sqrt{\mu}} \right) \tilde{\mathbf{R}}_1(t) + \left(A_1 \frac{2}{\alpha \mu} \mathbf{v}'_m + A_3 \frac{\mathbf{r}_m}{\sqrt{\mu}} \right) \frac{\partial \mathbf{v}'_m}{\partial \mathbf{v}_m} \tilde{\mathbf{V}}_1(t), \end{aligned} \quad (\text{A.7})$$

$$\begin{aligned} \frac{\partial f_2}{\partial \mathbf{v}_0} &= F_4(A_1, A_2, A_3) \\ &= \left(A_1 \frac{2}{\alpha r_m^3} \mathbf{r}_m + A_2 \frac{\mathbf{r}_m}{r_m} + A_3 \frac{\mathbf{v}'_m}{\sqrt{\mu}} \right) \mathbf{R}_1(t) + \left(A_1 \frac{2}{\alpha \mu} \mathbf{v}'_m + A_3 \frac{\mathbf{r}_m}{\sqrt{\mu}} \right) \frac{\partial \mathbf{v}'_m}{\partial \mathbf{v}_m} \mathbf{V}_1(t), \end{aligned} \quad (\text{A.8})$$

where $\frac{\partial \mathbf{v}'_m}{\partial v_m} = \mathbf{I}_{3 \times 3} \left(1 + \frac{\Delta v}{v_m} \right) + \frac{\Delta v}{v_m^3} \mathbf{v}_m \mathbf{1}_3^T$.

In the same way, we can obtain that $\frac{\partial g_2}{\partial \Delta v} = F_1(B_1, B_3)$, $\frac{\partial g_2}{\partial t_m} = -\dot{g}_2 + F_2(B_1, B_2, B_3)$,

$$\frac{\partial g_2}{\partial \mathbf{r}_0} = F_3(B_1, B_2, B_3), \quad \frac{\partial g_2}{\partial \mathbf{v}_0} = F_4(B_1, B_2, B_3), \quad \frac{\partial \dot{f}_2}{\partial \Delta v} = F_1(\dot{A}_1, \dot{A}_3), \quad \frac{\partial \dot{f}_2}{\partial t_m} = -\dot{f}_2 +$$

$$F_2(\dot{A}_1, \dot{A}_2, \dot{A}_3), \frac{\partial \dot{f}_2}{\partial \mathbf{r}_0} = F_3(\dot{A}_1, \dot{A}_2, \dot{A}_3), \frac{\partial \dot{f}_2}{\partial \mathbf{v}_0} = F_4(\dot{A}_1, \dot{A}_2, \dot{A}_3), \frac{\partial \dot{g}_2}{\partial \Delta v} = F_1(\dot{B}_1, \dot{B}_3),$$

$$\frac{\partial \dot{g}_2}{\partial t_m} = -\ddot{g}_2 + F_2(\dot{B}_1, \dot{B}_2, \dot{B}_3), \frac{\partial \dot{g}_2}{\partial \mathbf{r}_0} = F_3(\dot{B}_1, \dot{B}_2, \dot{B}_3), \frac{\partial \dot{g}_2}{\partial \mathbf{v}_0} = F_4(\dot{B}_1, \dot{B}_2, \dot{B}_3).$$

References

- Bar-Shalom, Y., Daum, F., & Huang, J. 2009, IEEE Control Systems Magazine, 29, 82
- Benoudnine, H., Keche, M., Ouamri, A., & Woolfson, M. S. 2012, IEEE Transactions on Aerospace Electronic Systems, 48, 197
- Der, G. J. 1997, Journal of the Astronautical Sciences, 45, 371
- Farnocchia, D., Tommei, G., Milani, A., & Rossi, A. 2010, Celestial Mechanics and Dynamical Astronomy, 107, 169
- Figueiredo, M. A. T., Nowak, R. D., & Wright, S. J. 2007, IEEE Journal of Selected Topics in Signal Processing, 1, 586
- Fortmann, T., Bar-Shalom, Y., & Scheffe, M. 1983, IEEE Journal of Oceanic Engineering, 8, 173
- Holzinger, M. J., & Scheeres, D. J. 2010, in Proceedings of the Advanced Maui Optical and Space Surveillance Technologies Conference, eds. S. Ryan, & The Maui Economic Development Board., 26
- Kelecy, T., & Jah, M. 2010, Acta Astronautica, 66, 798
- Lobo, M. S., Vandenberghe, L., Boyd, S., & Lebret, H. 1998, Linear Algebra and its Applications, 284, 193
- Maruskin, J. M., Scheeres, D. J., & Alfriend, K. T. 2009, Journal of Guidance, Control, and Dynamics, 32, 194
- Patera, R. P. 2008, Journal of Spacecraft and Rockets, 45, 554
- Petropoulos, A. E. 2005, 5th AAS/AIAA Space Flight Mechanics Conference, Copper Mountain, Colorado
- Sidi, M. J. 1997, Spacecraft Dynamics and Control: a Practical Engineering Approach, 7 (Cambridge: Cambridge Univ. Press)
- Storch, T. R. 2005, Master Thesis, Air Force Inst of Tech Wright-Patterson AFB OH School of Engineering And Management
- Tommei, G., Milani, A., & Rossi, A. 2007, Celestial Mechanics and Dynamical Astronomy, 97, 289